Identification of Ubiquitin Variants That Inhibit the E2 Ubiquitin Conjugating Enzyme, Ube2k

Adam J. Middleton,* Joan Teyra, Jingyi Zhu, Sachdev S. Sidhu, and Catherine L. Day

Read Online

ACCESS | Metrics & More | Article Recommendations | SI Supporting Information

ABSTRACT: Transfer of ubiquitin to substrate proteins regulates most processes in eukaryotic cells. E2 enzymes are a central component of the ubiquitin machinery, and generally determine the type of ubiquitin signal generated and thus the ultimate fate of substrate proteins. The E2, Ube2k, specifically builds degradative ubiquitin chains on diverse substrates. Here we have identified protein-based reagents, called ubiquitin variants (UbVs), that bind tightly and specifically to Ube2k. Crystal structures reveal that the UbVs bind to the E2 enzyme at a hydrophobic cleft that is distinct from the active site and previously identified ubiquitin binding sites. We demonstrate that the UbVs are potent inhibitors of Ube2k and block both ubiquitin charging of the E2 enzyme and E3-catalyzed ubiquitin transfer. The binding site of the UbVs suggests they directly clash with the ubiquitin activating enzyme, while potentially disrupting interactions with E3 ligases via allosteric effects. Our data reveal the first protein-based inhibitors of Ube2k and unveil a hydrophobic groove that could be an effective target for inhibiting Ube2k and other E2 enzymes.
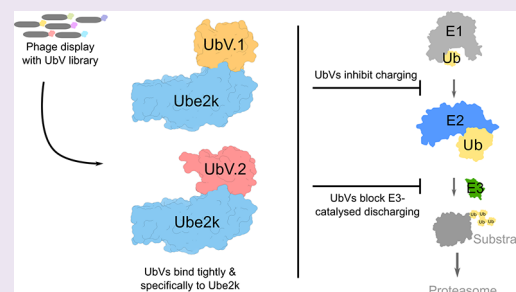
INTRODUCTION

Ubiquitin transfer is a post-translational modification that plays a critical role in almost all aspects of eukaryotic cells, including control of protein degradation by the proteasome,[1] modulation of gene expression,[2] recruitment of proteins to signaling platforms,[3,4] and dictation of the precise timing of cell division.[5] Consequently, dysregulation of ubiquitin transfer results in many diseases, such as cancers, immune disorders, and neurodegenerative diseases.[6] As a result, the ability to manipulate the components of the ubiquitin system is of considerable interest for the treatment of diseases.

Ubiquitin transfer is governed by three families of enzymes: the E1 ubiquitin activating enzymes, the E2 ubiquitin conjugating enzymes, and the E3 ubiquitin ligase enzymes.[7] Together, the machinery covalently links ubiquitin to a substrate lysine or N-terminal methionine residue with an isopeptide bond. Ubiquitin itself can be a substrate as it contains seven Lys residues, and this results in the formation of ubiquitin chains with distinct consequences.[8] For example, chains linked by Lys63 can act as scaffolds for recruiting proteins to signaling cascades, whereas Lys48-linked ubiquitin chains typically result in degradation of the attached substrate by the proteasome.[8] In the presence of RING E3 ligases, the nature of the ubiquitin signal is typically dictated by the E2 enzyme, of which there are ~40 in humans. Depending on their structure and biological context, E2 enzymes can add a single ubiquitin moiety or ubiquitin chains of various types to substrate proteins. Because the downstream effects of ubiquitin transfer are entirely dependent on the nature of the ubiquitin signal, E2 enzymes have a central role in ensuring that

substrate proteins are correctly modified by the ubiquitin machinery.

E2 enzymes are characterized by a conserved ubiquitin conjugating domain (UBC) that interacts with an E1 enzyme and E3 ligase via conserved and partly overlapping interfaces. After charging of the E2 enzyme with ubiquitin, the resulting E2∼Ub conjugate disengages the E1 and interacts with one of the hundreds of E3 ligases. The E3 ligase typically coordinates the choice of substrate to be modified, while also activating the E2∼Ub bond so that it is susceptible to nucleophilic attack.[9−13] When activated, the conjugated donor ubiquitin makes extensive contacts with the E2 enzyme, including nestling of ubiquitin's flexible C-terminal tail into a shallow groove of the E2 enzyme. When building ubiquitin chains, the E2 enzyme must also interact with a substrate ubiquitin, and this is referred to as the acceptor ubiquitin. Disrupting any of these protein–protein interactions can disable the E2 enzyme.

The ubiquitin conjugating enzyme, Ube2k, produces Lys48-linked ubiquitin chains exclusively and promotes the degradation of its targets in cells.[14] A recent report indicates that Ube2k is involved in promoting the degradation of the pro-survival Bcl-2 protein family member Mcl-1, suggesting

that Ube2k may have a pro-apoptotic role.[15] Other studies suggest that Ube2k is involved in overcoming cell-cycle arrest in response to DNA damage by promoting the degradation of p53.[16] In addition, Ube2k levels contribute to multiple neurodegenerative diseases that are characterized by the aggregation of proteins. For example, Ube2k is involved in Huntington's disease,[17] is associated with cell death from polyglutamine diseases,[18] is proapoptotic in response to the accumulation of amyloid-β,[19] and is elevated in the brains of individuals with schizophrenia.[20] Recent work suggests that Ube2k deficiency results in motor impairment reminiscent of Parkinson's disease and could act as a biomarker of the disease.[21] There is also evidence that Ube2k can add Lys48-linked chains onto already established Lys63 ubiquitin chains and thereby quench Lys63-induced signaling.[22] While the roles of Ube2k are diverse, they are unified by the ability of Ube2k to promote the degradation of substrate proteins. Development of inhibitors or activators that specifically target Ube2k would not only provide tools to allow a greater understanding of its function but may also provide a framework for small-molecule design.

Here, we have used a phage-displayed ubiquitin variant (UbV) library to isolate specific inhibitors of Ube2k. Of the six UbV binders identified, two are potent inhibitors of ubiquitin transfer promoted by Ube2k. Biochemical experiments demonstrate that both UbVs inhibit charging of Ube2k by the E1 enzyme and also E3-catalyzed discharge. Structures of the UbV−Ube2k complexes show that both UbVs bind in a hydrophobic cleft distant from the active site, and this site includes E2−E1 contacts. While this explains why charging of Ube2k is impeded, the UbV binding site does not overlap with the E3-binding site, and the reason for decreased E3-catalyzed discharge is less certain. Our research reveals a hydrophobic groove on Ube2k that can bind ligands to block the assembly of degradative ubiquitin chains.

RESULTS AND DISCUSSION

Selection of UbVs That Bind Ube2k. To discover specific modulators of the E2 enzyme Ube2k, we used a highly diverse phage-displayed library containing 2×10^9 unique UbVs. The library was a further iteration of libraries generated for selection against deubiquitinases, E3 ligases, and other E2 enzymes.[23−25] In this library, residues were diversified across the surface of ubiquitin that is involved in the vast majority of ubiquitin−protein interactions, including contacts with E2s, ubiquitin-associating domains, and deubiquitinases. The surface comprises the β sheet of ubiquitin and its five flexible C-terminal residues (Figure 1A). To minimize disruptions to the fold of ubiquitin while maximizing diversity across the surface, the library was built using a "soft-randomization" approach with degenerate codons that encode for approximately 50% wild-type sequence at each diversified position.[26]

Ube2k has a C-terminal extension that contains a ubiquitin associating (UBA) domain,[27] which binds ubiquitin but is dispensable for ubiquitin transfer *in vitro*. As our goal was to identify modulators of ubiquitin transfer, we generated a truncated Ube2k construct that comprised only the UBC domain (Ube2k−UBC). To enable us to isolate UbVs that could bind to either Ube2k, ubiquitin, or the E2-ubiquitin interface, we prepared a stable isopeptide linked Ube2k^k−UBC~Ub conjugate. This was achieved by mutating the active site cysteine to lysine (C92K) in Ube2k−UBC and inclusion of a C-terminal AVI tag to enable specific biotinylation (Figure
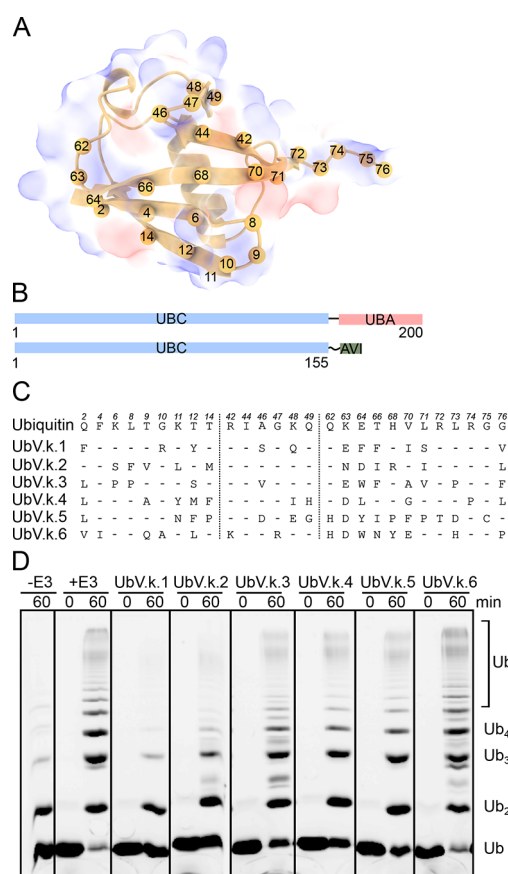
Figure 1. Selection for UbVs that bind to Ube2k. (A) The structure of wild-type ubiquitin (1UBQ) with the diversified residues shown as numbered spheres. Ubiquitin shown as a cartoon against a semitransparent surface with acidic, basic, and hydrophobic groups colored red, blue, or white, respectively. (B) Domain structure of full-length Ube2k and Ube2k−UBC used in this study. UBC, ubiquitin conjugating domain; UBA, ubiquitin associated domain; AVI, biotin-specific tag. (C) Sequence alignment of wild-type ubiquitin and the UbVs isolated from the selection. Only regions diversified in the library are shown. In the alignment, the amino acids indicate changes relative to the wild-type ubiquitin sequence, while dashes represent no change. (D) Chain-building ubiquitin (Ub) transfer assay performed without (−E3 and +E3) and with (+E3) the six UbVs (at a final concentration of 30 μM). In this assay, Ube2k was at 10 μM, and the E3 ligase RNF125 (at 10 μM) was used to promote ubiquitin transfer. Imaged as fluorescence from 5AIF-tagged ubiquitin. Assay performed in triplicate with similar results.

1B). After purification and biotinylation of Ube2k^k−UBC, the E2 enzyme was charged with ubiquitin to generate a stable Ube2k^k−UBC~Ub conjugate, further purified, then immobilized to streptavidin/neutravidin-coated wells for phage-display selections.

After five rounds of phage-display selections against Ube2k^k−UBC~Ub, clones were sequenced, and six unique UbVs were chosen for closer analysis (Figure 1C). Each UbV (including an N-terminal FLAG tag) was subcloned into a vector that encoded a cleavable N-terminal His tag, and the resulting UbVs were expressed in *Escherchia coli*. After purification, interaction of each UbV with Ube2k^k−UBC~Ub was confirmed using an ELISA experiment (Figure S1A). Importantly, the ELISAs showed that each UbV bound to Ube2k and Ube2k^k−UBC~Ub with comparable affinity but did not bind ubiquitin alone. This indicated that the UbVs
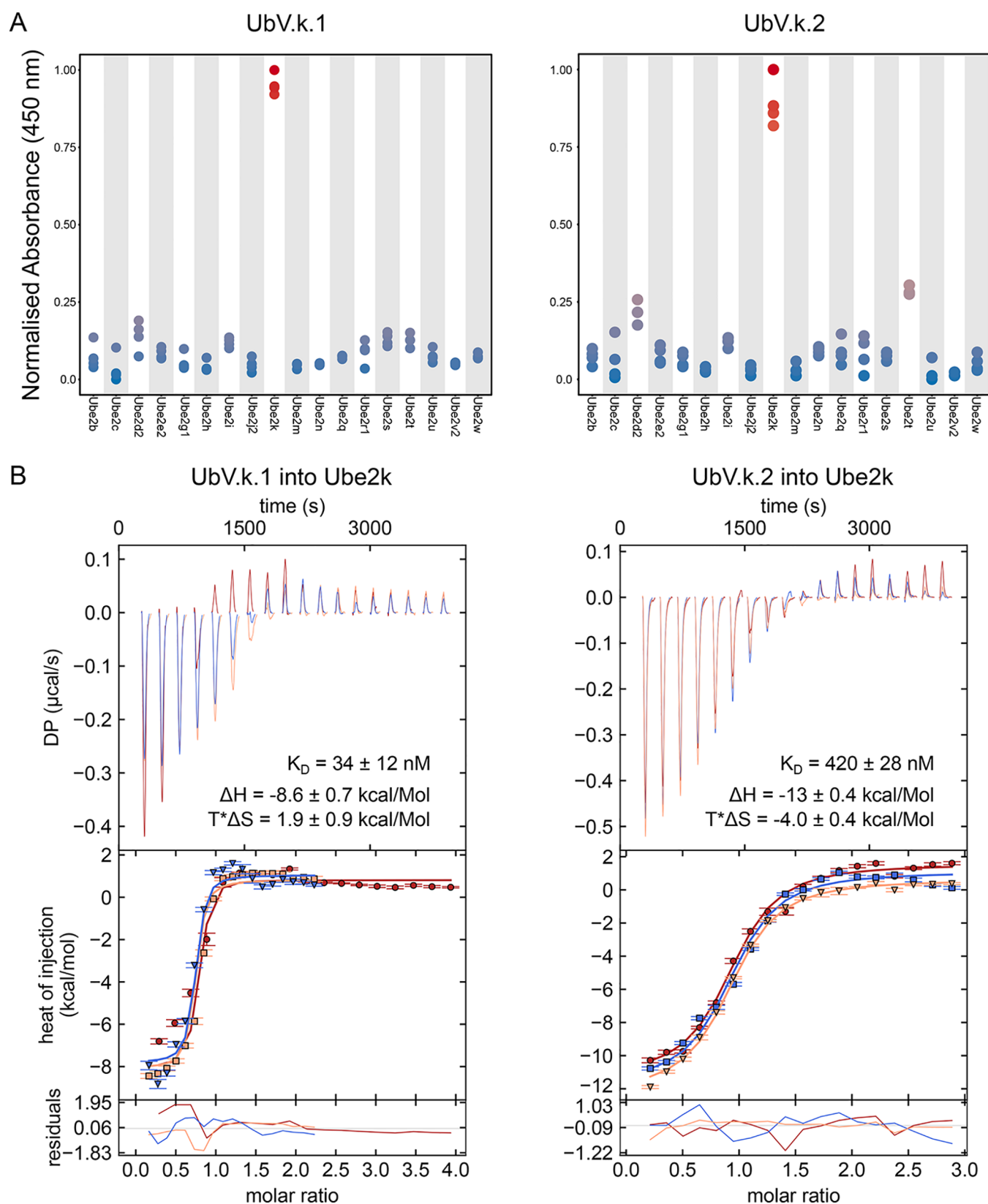
Figure 2. The UbVs bind to Ube2k specifically and tightly. (A) E2 enzyme specificity screen was performed using ELISA. A representative panel of E2 enzymes was immobilized to a plate before the UbVs were added, and binding was detected spectrophotometrically by absorbance at 450 nm. Readings were normalized, and four replicates were performed. (B) Thermograms (top) and fitted isotherms (bottom) of ITC measurements performed in technical triplicate (shown in blue, red, and orange) where either UbV.k.1 or UbV.k.2 was injected into Ube2k. Mean thermodynamics (K_D, ΔH, and $T*\Delta S$) are from three technical replicates, while the error represents SEM.

targeted Ube2k. The effect of each UbV on ubiquitin transfer was then assessed using a chain-building assay in the presence of Ube2k (Figure 1D). For this assay, each component of the ubiquitin cascade (E1, E2, E3, ubiquitin, and ATP) was mixed together and incubated at 37 °C prior to analysis. In this experiment, five of the UbVs (UbV.k.1−5 Figure 1C,D) decreased ubiquitin chain assembly by Ube2k, with UbV.k.1 and UbV.k.2 being the most potent inhibitors. As a result, we focused our attention on these two UbVs.

The UbVs Bind Tightly and Specifically to Ube2k. The UBC domain of E2 enzymes is structurally conserved, and while there is less conservation on a sequence level, there is the possibility that the UbVs that bind and inhibit Ube2k might cross-react with other E2s. To measure specificity, we assessed binding of UbV.k.1 and UbV.k.2 to a representative panel of 18 E2 enzymes. Our results revealed preferential binding of both UbVs for Ube2k, with minimal binding to other E2 enzymes (Figure 2A). In support of this, no inhibition was seen when chain building assays were performed with two other E2 enzymes, Ube2d2 and Ube2n/Ube2v2, in the presence of the UbVs (Figure S1B).

Next, we performed ITC to quantitatively measure the interaction between the UbVs and Ube2k. Each UbV was titrated against full-length Ube2k as well as Ube2k−UBC. The K_D of UbV.k.1 for Ube2k was calculated to be 34 nM (Figure 2B), while UbV.k.2 bound to Ube2k approximately 10-fold weaker, with a calculated K_D of 420 nM (Figure 2B). Similar dissociation constants were observed for both UbVs with Ube2k−UBC (Figure S2A), suggesting that the UbVs interacted with the UBC domain and not the UBA domain. Additionally, comparable dissociation constants were obtained when titrating the UbVs against Ube2k^k−UBC∼Ub, suggesting that binding of the UbVs to Ube2k is not hindered (or promoted) when the E2 is conjugated with ubiquitin (S2B, S2C). In further support of a stable interaction, thermal denaturation experiments demonstrated that the melting temperature of Ube2k was increased by 4 or 2 °C in the presence of UbV.k.1 or UbV.k.2, respectively (Figure S2D). Together, these results demonstrate that the inhibitory UbVs are highly specific for Ube2k, bind tightly to the E2 enzyme, and increase the E2's stability.

The UbVs Inhibit Charging and Discharging of Ube2k. What remained unclear was how the UbVs can block ubiquitin transfer from Ube2k. To promote ubiquitin transfer, E2 enzymes must first be loaded with ubiquitin by an E1 enzyme, which transfers ubiquitin to the E2 in a transthiolation reaction. The E2∼Ub conjugate then disengages from the E1 enzyme and binds an E3 ligase that catalyzes ubiquitin transfer.[28] The chain-building assay (Figure 1D) involves both charging of the E2 by an E1 enzyme and E3-dependent ubiquitin transfer. To tease out the mechanism of inhibition, we analyzed E1-dependent charging and E3-catalyzed transfer separately. First, to determine if the UbVs affected charging of Ube2k, we monitored the formation of an E2∼Ub thioester linked conjugate in the absence or presence of the UbVs. As observed in Figure 3A, both UbVs impeded charging of Ube2k as judged by slowed formation of an E2∼Ub species over time, with UbV.k.1 being a more potent inhibitor than UbV.k.2 (Figure 3A). We also confirmed that the UbVs did not affect the upstream E1 activation of ubiquitin (Figure S3). These results suggest that the UbVs impede loading of Ube2k by the E1 enzyme.
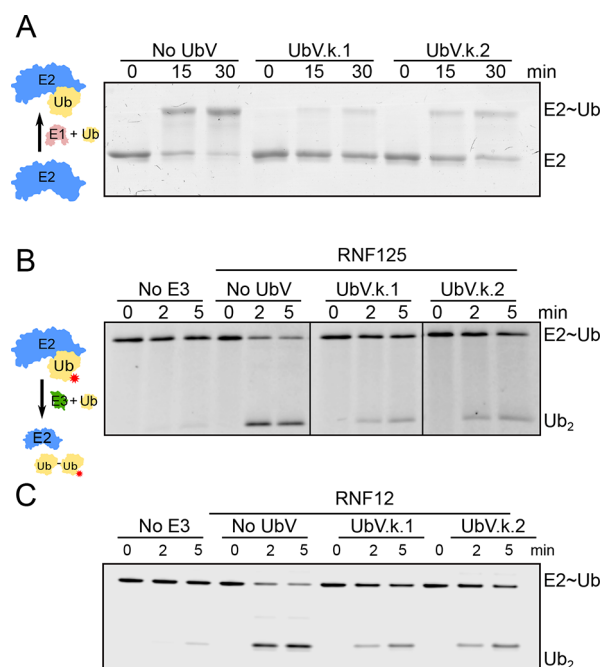
Figure 3. The UbVs inhibit both E2 charging and E3-catalyzed ubiquitin discharge. (A) E2 charging assay (see schematic on the left) performed with and without the UbVs. Samples were quenched with nonreducing dye at the indicated time points. Ube2k was at a final concentration of 10 μM, ubiquitin at 50 μM, UbVs at 10 μM, and E1 at 0.1 μM. The gel was visualized by staining with Coomassie blue dye. (B, C) A ubiquitin discharge experiment (schematic on the left; red star indicates fluorescent tag) performed with and without the UbVs. The Ube2k∼Ub^{K0}−Cy3 was at a final concentration of 2 μM, while the UbVs were at 10 μM. Samples were quenched with nonreducing dye at the indicated time points. The gel was imaged by fluorescence detected at 600 nm. Panels B and C show results with RNF125 (final concentration of 0.25 μM) or RNF12 (2.5 μM) as the E3 ligase, respectively.

To assess whether the UbVs could also inhibit E3-catalyzed ubiquitin transfer from Ube2k, we prepared a fluorescently tagged thioester-linked Ube2k∼Ub−Cy3^{K0} conjugate and monitored the disappearance of the conjugate and appearance of diubiquitin in the presence of an E3 ligase and excess UbVs (Figure 3B,C). Our results show that the E3-dependent discharge was slowed by the UbVs when using either RNF125 or RNF12 E3 ligases. However, in the absence of an E3 ligase, the UbVs did not affect the basal ubiquitin transfer activity of Ube2k (Figure S4). These results suggest that, as well as inhibiting charging of the E2 enzymes by the E1 enzyme, the UbVs also disrupted E3 ligase catalyzed ubiquitin discharge.

Structures of the UbV−Ube2k Complexes Reveal the Mechanism of Inhibition. To establish exactly how the two UbVs bind and inhibit the activity of Ube2k, we solved their structures in complex with the E2 enzyme. Following copurification of UbV.k.2 and Ube2k, crystals were obtained for the complex, and its structure was solved by molecular replacement using Ube2k and ubiquitin. The structure was refined to a resolution of 2.4 Å with a final R_{work}/R_{free} of 20.6/24.9 (Table 1). Crystals of a similarly purified UbV.k.1−Ube2k complex could not be obtained. Instead, we purified an isopeptide-linked Ube2k^k∼Ub conjugate and copurified it with UbV.k.1. With this complex, crystals were obtained, and the structure of UbV.k.1−Ube2k^k∼Ub was solved to 3.0 Å with a

Table 1. Crystallographic Data Collection and Refinement Statistics

	UbV.k.1−Ube2k^k∼Ub	UbV.k.2−Ube2k
PDB entry	7MYF^a	7MYH
	data collection	
wavelength (Å)	0.9537	0.9537
beamline	Australian synchrotron MX2	Australian synchrotron MX1
resolution range	33.8−3.00 (3.1−3.0)^b	38.0−2.39 (2.48−2.39)
space group	I121	P212121
	unit cell dimensions	
a, b, c (Å)	89.14, 37.79, 117.8	38.84, 76.09, 135.48
α, β, γ (deg)	90, 98.27, 90	90, 90, 90
total no. of reflections	36340 (5956)	91231 (9474)
unique reflections	7782 (800)	16395 (1565)
multiplicity	4.6 (4.6)	5.5 (5.8)
completeness (%)	96.3 (99.1)	99.2 (97.1)
R_{merge}	0.17 (0.83)	0.09 (1.40)
I/σ (I)	6.2 (1.9)	12.8 (1.2)
$CC_{1/2}$	0.991 (0.683)	0.999 (0.551)
	refinement	
average B factor (Å^2)	75.9	61.6
no. of reflections	7778 (800)	16386 (1564)
no. of reflections (free)	406 (55)	807 (80)
R_{work} (%)	23.7 (32.6)	20.8 (32.0)
R_{free} (%)	29.1 (43.4)	25.2 (37.7)
no. of atoms	2707	2197
protein	2707	2167
solvent	0	24
ligand	0	6
RMSD bonds (Å)	1.01	1.25
RMSD angles (deg)	0.004	0.009
favored (%)	93.4	95.6
allowed (%)	6.6	4.4
outliers (%)	0	0

^{a}Each structure was determined from a single crystal. ^{b}Values for the highest-resolution shell are shown in parentheses.

final R_{work}/R_{free} of 23.4/29.3 (Table 1). In both cases, the asymmetric unit contained only one complex.

In both structures, Ube2k shows the expected fold comprising a UBC domain bridged by a short linker to a C-terminal UBA domain (Figure S5A,B). A C-alpha overlay of Ube2k from the two structures has an RMSD of 1.2 Å, and they both overlay well with a published structure of Ube2k (PDB: 5DFL)[29] with C-alpha RMSDs of 1.3 and 0.65 Å for Ube2k−UbV.k.1 and −UbV.k.2, respectively. In the Ube2k−UbV.k.2 complex, residues 32−34 of Ube2k and 7−12 of UbV.k.2 are shifted toward each other, and it appears that a slight conformational change of both proteins is necessary to form the complex.

Both UbVs bind at the same position of Ube2k, which comprises a hydrophobic cleft formed between α-helix 1 and β-sheet 1 of Ube2k (Figure 4A,B). Surprisingly, an overlay of the two complexes shows that the UbVs are rotated by approximately 15° with respect to one another and Ube2k (S5B), even though the contact residues from both are largely from the same sequence positions. Notably, the contact residues from both UbVs are part of the diversified surface, with major contributions from those mutated from wild-type ubiquitin (Figure 1B, Figure 4C, D, E). An analysis of

symmetry mates in the crystal structure shows that UbV.k.1 makes extensive contacts with a neighboring Ube2k molecule and two ubiquitin molecules. These interactions appear to be critical crystal contacts, but they are unlikely to contribute to the primary UbV.k.1−Ube2k interaction. By contrast, UbV.k.2 makes only minor contacts with neighboring molecules. An analysis using PISA (Protein, Interfaces, Structures, and Assemblies)[30] reveals that the interface between UbV.k.1 and Ube2k buries approximately 470 Å^2, while UbV.k.2 buries approximately 530 Å^2. While both UbVs bury a modest surface, they both bind with submicromolar affinity. UbV.k.1 has much higher affinity for Ube2k (K_D of ∼30 nM vs ∼420 nM), and the ITC results (Figure 2 and Figure S2A,B) show that the difference in affinity is entropy driven. Indeed, this difference is reflected in the larger hydrophobic patch buried in the UbV.k.1−Ube2k interaction (Figure 4E,F).

The more potent UbV, UbV.k.1, uses an array of four Phe residues (Phe2, Phe4*, Phe64, and Phe66; wild-type ubiquitin residues are indicated with asterisks) and one Tyr residue (Tyr12) to form a hydrophobic surface that packs against Ube2k residues Phe13, Leu17, Leu31, and Phe36 (Figure 4C,F). This patch is complemented by a hydrophilic "shell" made up of the hydroxyls of Tyr12 and Thr14*; the side chain Glu63 of UbV.k.1; and Lys10, Lys14, Asp30, and Glu34 of Ube2k (Figure 4C,F). In a similar manner, the UbV.k.2−Ube2k interaction has a hydrophobic core, comprising Phe4*, Phe8, and Ile66 of UbV.k.2, which interacts with the same patch on Ube2k as for UbV.k.1 (Phe13, Leu17, Leu31, and Phe36). This is supported by an extensive polar shell nucleated by Ser6 of UbV.k.2, which acts to stabilize contacts between Thr12* of UbV.k.2 with Asp30 and Leu31 of Ube2k (Figure 4D,F). In addition, the side chain of Lys14 of Ube2k contacts Gln2* and Asp64 of UbV.k.2, while the side chain of Lys28 of Ube2k makes contacts with Gly10*.

To test the importance of the diversified residues, we introduced single point mutations to revert both UbVs to the wild-type ubiquitin sequence and assessed binding of the mutants to Ube2k by ELISA EC_{50} measurements. Interestingly, each revertant disrupted the EC_{50} by at least an order of magnitude, while some of the mutations almost eliminated binding (Figure 5A,B). For UbV.k.1, mutation of Phe64 and Glu63 to their wild-type amino acids (Glu and Lys, respectively) almost completely disrupted binding to Ube2k, while for UbV.k.2, mutating Ser6 to Lys as well as Ile66 to Thr was highly disruptive to binding. In support of the importance of these residues, the mutations F64E and E63K made to UbV.k.1, as well as S6K and I66T on UbV.k.2, did not inhibit the formation of ubiquitin chains (Figure 5C). These data suggest that the network of diversified residues is highly interdependent, and disruption of any of them results in a notable loss of binding and inhibition.

Architecture of UbV−Ube2k Interactions. Ubiquitin activation by an E1 enzyme sets the stage for subsequent transfer to E2 enzymes and E3-ligase catalyzed ubiquitin transfer. The E1 enzyme engages E2s using two major interactions: first, the E2 enzyme is recruited by a ubiquitin-fold domain (UFD) that interacts with a semiconserved surface on E2s; subsequently, the UFD domain rotates and positions the active site domain of the E1 next to the catalytic Cys of the E2 enzyme to allow a transthiolation reaction to occur.[31,32] Because there is no structure of Ube2k bound to the E1, we generated a molecular model by overlaying Ube2k from our two structures with Cdc34 from a recent E2−E1 complex
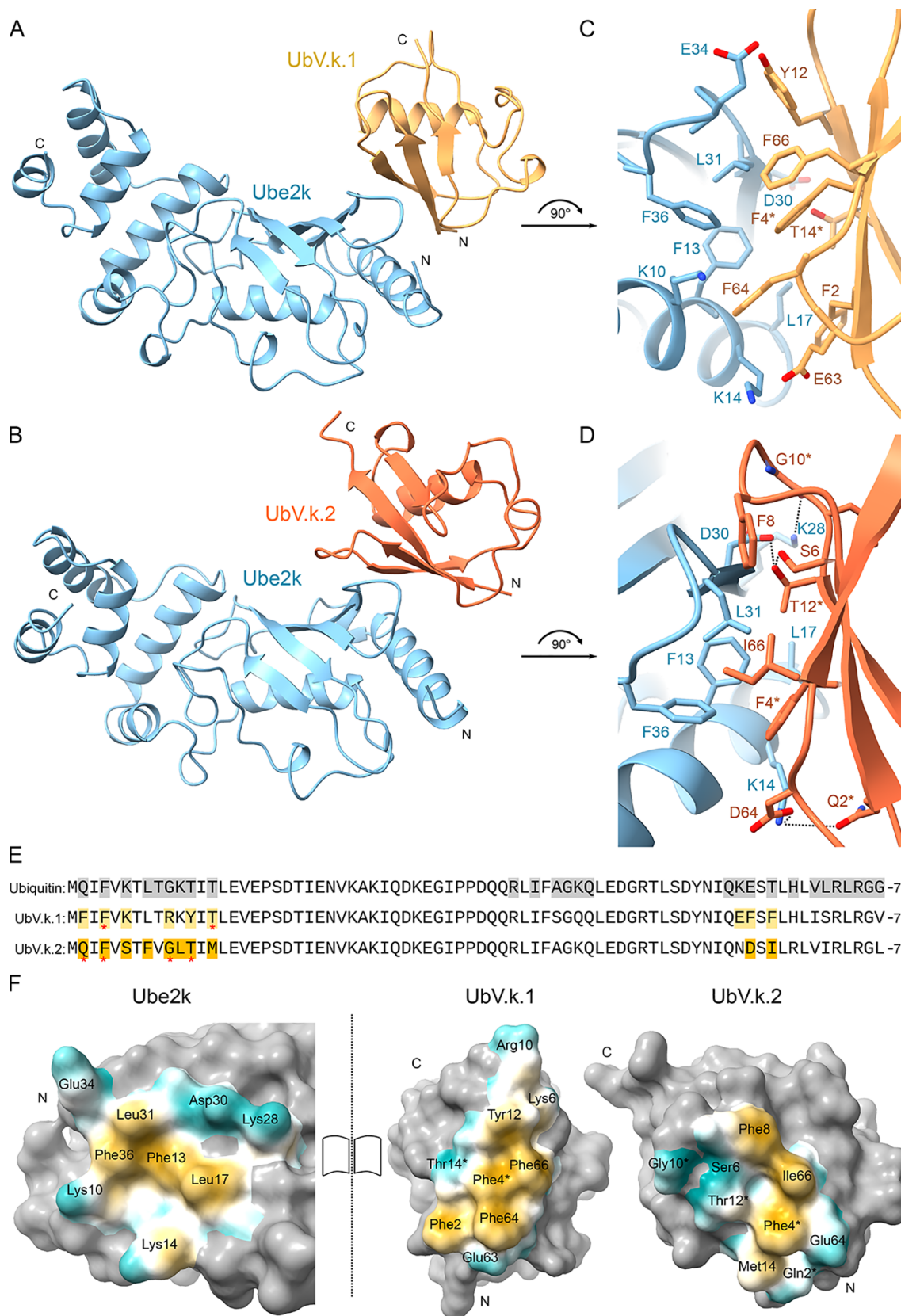
Figure 4. Crystal structures of UbV.k.1 or UbV.k.2 in complex with Ube2k. (A,B) Ribbon representation of UbV.k.1 (A) or UbV.k.2 (B) in complex with Ube2k. N and C termini are labeled. The full structure of the UbV.k.1−Ube2k^k∼Ub complex including the conjugated ubiquitin is shown in Figure S5A. (C, D) Close-up views of the interfaces between the UbVs and Ube2k. The main chains are shown as ribbons, and side chains are shown as sticks colored as in panels A and B. Dashed lines indicate predicted hydrogen bonds. Residues unchanged from wild-type ubiquitin are indicated with asterisks. (E) Sequence alignment of wild-type ubiquitin, UbV.k.1, and UbV.k.2 with the residues that contact Ube2k highlighted. Red asterisks indicate residues that are unchanged from wild-type ubiquitin. (F) Open book representation of the UbV−Ube2k

Figure 4. continued

interactions. On the left is Ube2k from both complexes, while UbV.k.1 and UbV.k.2 are shown on the right. Noncontact residues are shown in gray, while contact residues are colored based on their molecular lipophilicity potential: hydrophobic atoms are colored orange, while hydrophilic atoms are cyan. Residues unchanged from wild-type ubiquitin are indicated with asterisks.

structure and mapped the predicted UFD contacts on Ube2k (Figure 6A). In our model, both the UbVs clash with the predicted binding site of the UFD, likely explaining why ubiquitin charging of Ube2k by the E1 enzyme is reduced in the presence of the inhibitory UbVs.

The UbVs also disrupt the activity of E3-catalyzed discharge of Ube2k (Figure 3B,C). Because neither UbV inhibited the basal discharge of Ube2k (Figure S4), we presume that the UbVs disrupt E3-catalyzed discharge. Overlay of Ube2k from the Ube2k−UbV.k.1 complex with Ube2d2 from a crystal structure of Ube2d2-RNF12 (Figure 6B)[33] showed that there is no overlap between RNF12 and the UbVs. It is therefore unlikely that inhibition of E3-catalyzed discharge of Ube2k is due to steric hindrance. Instead, the UbVs likely serve as allosteric regulators of ubiquitin transfer. Allosteric regulation of E2 enzymes has been observed before. For example, the Ube2d family of E2 enzymes is activated by binding of a noncovalent ubiquitin molecule distant from the active site.[34] Furthermore, a small molecule allosteric regulator of the E2 enzyme Cdc34 has been reported to disrupt ubiquitin transfer to substrates.[35] In summary, the architecture of both the UbV−Ube2k interactions suggests a direct steric clash with the E1 enzyme, while the mechanism of inhibition of E3 ligases by the UbVs is most likely due to allosteric effects. Additional structural analysis of E3-ligase-bound Ube2k complexes will be needed to reveal the molecular details of ubiquitin transfer by Ube2k.

Conclusions. As the central enzymes in the ubiquitin cascade, E2 enzymes play a critical role in determining the exact nature of the ubiquitin code.[3] Here, we have focused on developing tools to modulate targeting of proteins to the proteasome by identifying regulators of the E2 enzyme, Ube2k, which only produces Lys48-linked degradative ubiquitin chains. Using phage display, we discovered two UbVs that are potent inhibitors of ubiquitin transfer by Ube2k. The UbVs bind tightly and highly specifically to Ube2k, and they appear to isolate the E2 from the ubiquitin system by disrupting interactions with both E3 ligases and the E1 enzyme. The fact that both UbVs bind at the same hydrophobic cleft on Ube2k suggests that this site may prove to be an effective target for small molecule binding. By inhibiting the synthesis of a degradative signal, these UbVs will provide tools for research and may suggest approaches for the design of small molecule Ube2k inhibitors. For example, the UbVs may prove useful for the discovery of small molecules that bind at this same hydrophobic cleft by displacement assays, as demonstrated by others.[36] While the biology on Ube2k suggests that increasing its activity may be desirable for treating many diseases, there remain cases where inhibiting its activity may be valuable.[16,18]
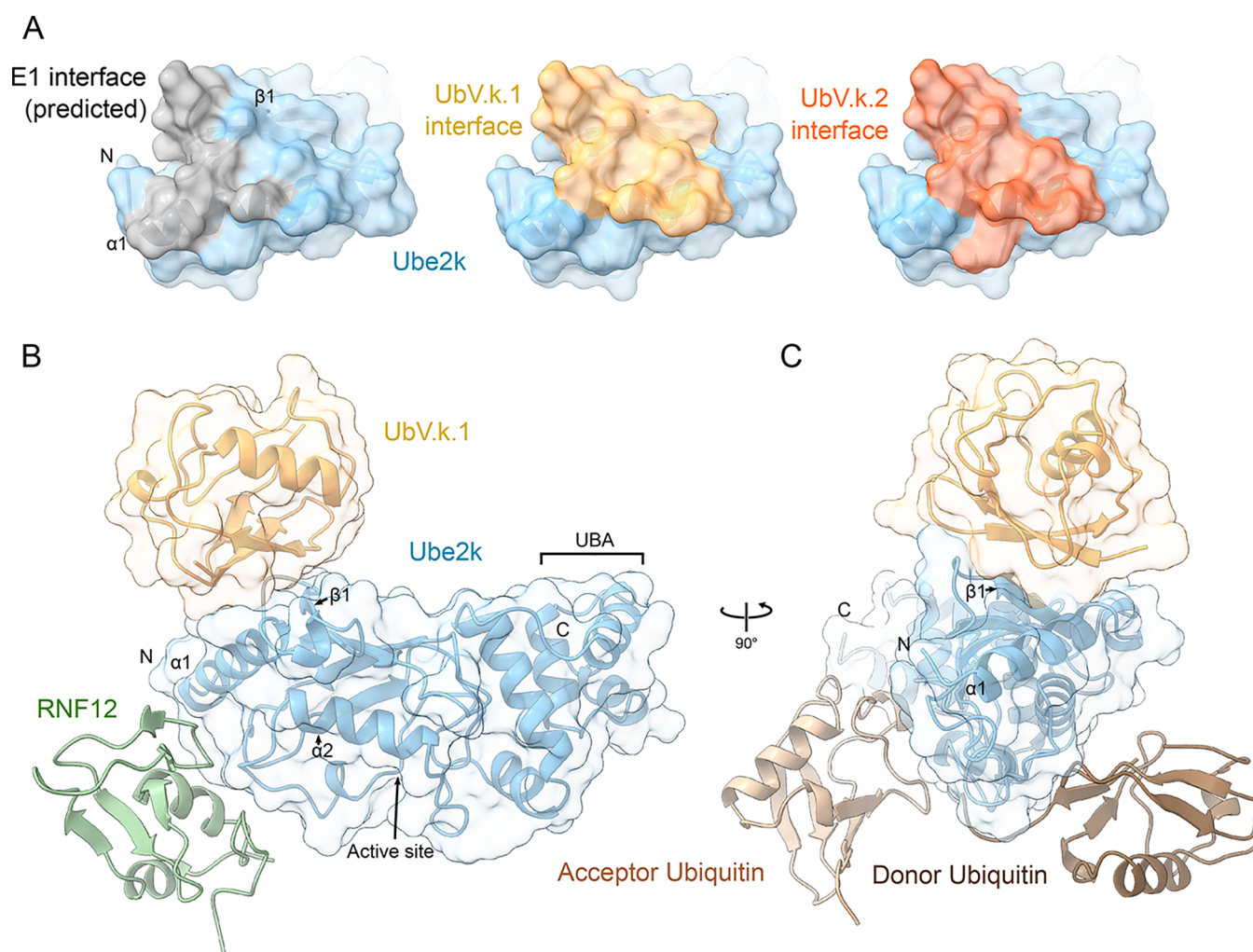
To date, approximately 20 inhibitors of ubiquitin-conjugating E2 enzymes have been discovered.[37−49,35] Many of the reported inhibitors target the active site Cys, others act by disrupting protein−protein interactions, and some have an allosteric effect on ubiquitin transfer. Because of the conservation and lack of a distinctive active site pocket on E2 enzymes, many of these orthosteric inhibitors have low specificity and relatively high IC_{50} values.[8] Display technolo-

gies offer powerful ways of isolating protein or peptide-based inhibitors of proteins (including E2 enzymes) that can circumvent these problems. For example, phage display was used to discover UbVs that bound at the "backside" ubiquitin binding site found on some E2 enzymes.[37] These variants bound more tightly than many other inhibitors of E2 enzymes, with IC_{50} measurements ranging from 65 to 280 nM. Importantly, they could all inhibit ubiquitin transfer by either directly blocking interactions with other components of the ubiquitin cascade (similar to what we observed here) or by allosteric effects that disrupt the enhanced ubiquitin transfer normally provided by backside-bound ubiquitin.

Surprisingly, the UbVs we discovered did not bind at a predicted ubiquitin-binding site (Figure 6C), nor did they block the active site Cys. Instead, they bound at a hydrophobic groove between α-helix 1 and β-sheet 1 on Ube2k that overlaps considerably with the binding site of the UFD domain of E1 enzymes (Figure 6A)[31,32,50,51] but binds in a distinct manner. The UFD−E2 interface appears to be largely governed by polar contacts between acidic residues on the E1 and a set of basic residues conserved on helix-1 of E2 enzymes. By contrast, both of the UbVs reported here rely on a hydrophobic patch, as well as critical polar contacts between the molecules (Figure 4C,D,F, Figure 5). A sequence comparison of the E2 enzymes used in our representative screen suggests that the residues of Ube2k that interact with the UbVs are not highly conserved (Figure S6). In particular, this is true for the hydrophobic residues, Phe13, Leu17, Leu31, and Phe36, which provide the core of both of the interactions. This low conservation likely explains the specificity of the interaction with Ube2k. How the UbVs block engagement by the E3 ligase is not as clear, because in our model (Figure 6B) the UbVs bind away from the predicted RNF12 binding site on Ube2k. E3 ligase−E2 interactions are highly conserved, and it is unlikely that the E3−Ube2k interaction will differ greatly from our model. As a result, it is probable that the inhibition of E3 ligase activity is due to allosteric effects caused by the UbV−Ube2k interactions.

Currently, the role of Ube2k in biology has not been extensively investigated, but studies have shown that the enzyme appears to have diverse roles in cells, such as regulating cell division,[52] controlling the stability of p53,[16] and is likely to play roles in the development of neurodegenerative diseases.[17−21] The UbVs may prove to be productive in narrowing down the exact importance of Ube2k in the cell. While there is considerable redundancy in the cell, Ube2k is the only E2 enzyme that contains a ubiquitin-binding domain, which may act to increase the local concentration of the enzyme to promote rapid synthesis of extensive ubiquitin chains and degradation. An interesting recent report suggests that the UBA domain may be involved in recruiting Ube2k to Lys63-linked ubiquitin chains to potentially quench signaling pathways promoted by Lys63 chains.[22] Further work is needed to understand more about the role of Ube2k in cells, and the UbVs may prove essential to these studies.

Figure 5. Single point mutations to UbVs are sufficient to decrease both Ube2k binding and inhibitory activity. (A,B) The binding of the UbVs and their mutants to Ube2k was detected using ELISA as in Figure 2A. UbV.k.1 and its mutants are shown in panel A, while UbV.k.2 and its mutants are in panel B. The EC_{50} values were calculated as the point where the absorption signal was 50% of the maximum. Errors in the EC_{50} values show the standard deviation from the dose−response curve. (C) Ubiquitin chain-building assay performed with or without the UbVs or revertants that fully disrupted binding. Ube2k and the UbVs were at 10 μM. Imaged as fluorescence from 5AIF-tagged ubiquitin.

■ METHODS

DNA Constructs. For phage selection, a DNA construct encoding residues 1−157 of Ube2k (Ube2k−UBC) containing the mutations C92K and K97R fused to a short GSGS linker and an AVI tag was

obtained from GeneArt (Invitrogen). This construct was used to generate a stable isopeptide-linked Ube2k^k~Ub conjugate. A DNA construct encoding the biotin ligase BirA was obtained from GeneArt. Both of these constructs were cloned into a pET-LIC vector encoding a 6xHis tag followed by a 3C protease cleavage site N-terminal to the construct. For the E2 specificity screen, a modified pET-LIC vector was constructed to allow coexpression of C-terminal AVI-tagged proteins with the biotin ligase BirA. This vector was named pET-LIC-AVI-BirA-Duet. For cloning of the E2s, primers containing LIC overhangs were used to amplify a representative panel of E2 enzymes, and these were then cloned into pET-LIC-AVI-BirA-Duet. Mutations were generated using single-step site-directed mutagenesis.[53] After phage selection, the DNA sequences encoding the UbVs were amplified using universal primers and cloned into pET-LIC. Cloned UbVs included an N-terminal FLAG tag and a C-terminal GGSGG tag. An RNF125 construct encoding residues 16−125 was cloned into pGEX-6P3 using *Bam*HI and *Eco*RI restriction digestion and ligation.

Protein Expression and Purification. Each protein was produced in the *E. coli* BL21-star cell line in LB broth by incubation at 37 °C followed by 18 °C for overnight expression. Protein expression was either induced by 0.2 mM IPTG or by autoinduction. After centrifugation, cell pellets were resuspended in 1× PBS, sonicated, and centrifuged at 15 000*g*. For constructs in the pET-LIC vector, the His-tagged protein was immobilized to nickel beads (Macherey-Nagel), eluted with 300 mM imidazole and either dialyzed or desalted into PBS. Subsequently, this was mixed with in-house produced His-tagged 3C for overnight digestion to remove the His tag. For purification of BirA, the 3C digestion was not performed. After confirmation of digestion, the protein was further purified using size-exclusion chromatography over a Superdex S75 10/300 or 16/600 column (GE Healthcare). For Ube2k−UBC containing the AVI tag, the purified protein was incubated at a final concentration of 100 μM with 300 μM biotin, 2 μM BirA, 2.5 mM ATP, and 2.5 mM MgCl$_2$ for 1 h at RT. To confirm biotinylation, the purified proteins were incubated with excess streptavidin (New England Biolabs) for 10 min before analysis via gel-shift using SDS-PAGE. The protein was then desalted to remove excess biotin, and the BirA removed using Ni^{2+} affinity chromatography. For the constructs in pET-LIC-Avi-BirA-Duet, a final concentration of 200 μM biotin was added to the *E. coli* cultures before transfer to 18 °C. Ubiquitin, E1, Ube2k, Ube2d2, Ube2n, Ube2v2, RNF12, TRAF6, and 3C protease were purified using previously established methods.[29,33,54−56] RNF125 was purified as described for RNF12. The RNF12 construct used comprised residues 530−624 as reported in reference 33. Ubiquitin with all Lys residues mutated to Arg (K0) was purified identically to wild-type ubiquitin. Thioester and isopeptide linked Ube2k~Ub/Ube2k^k−UBC~Ub were purified using techniques previously described.[57] Fluorescently labeled ubiquitin for chain-building assays (Ub-5AIF), ubiquitin discharge assays (Ub-Cy3^{K0}), and E1 activation assays (Ub-Cy3) were produced as previously described. GST-Ubiquitin and GST alone were purified by binding to GSH resin, and elution from the resin with 10 mM GSH for 30 min. Subsequently, they were purified by size-exclusion chromatography. All proteins were frozen in liquid nitrogen and kept at −80 °C.

Phage-Display Selections. Five rounds of phage-display selections were performed as previously described using a library highly similar to the ones used in earlier studies.[23,37] For selection, biotinylated Ube2k^k−UBC~Ub was immobilized to Nunc Maxisorp 96-well plates (Fisher Scientific) coated alternately with neutravidin (New England BioLabs) or streptavidin (ThermoFisher Scientific). After blocking, the UbV library was added to immobilized Ube2k^k−UBC~Ub for 1 h at 4 °C followed by washing with PBS containing 0.05% (v/v) Tween-20 and elution at low pH. Subsequently, *E. coli* TOP10 cells (ThermoFisher Scientific) were infected with the eluted phage before being grown overnight at 37 °C. The *E. coli* TOP10 cells were plated, and 96 individual clones (48 from round four and 48 from round five) were grown and sequenced. From the sequences, six distinct UbVs were analyzed in subsequent experiments.

Ubiquitin Transfer Assays. In order to minimize autoubiquity-lation of Ube2k, all assays were performed using a Ube2k variant

Figure 6. Molecular architecture of the Ube2k−UbV structures. (A) Surface representation of Ube2k showing residues predicted to be within 3 Å of the UFD domain of the E1 ubiquitin activating enzyme (left, in gray) and contacts with UbV.k.1 or UbV.k.2 (middle and right, in yellow or orange, respectively). Noncontacting Ube2k residues are shown in blue. (B) Model of RNF12-bound Ube2k was generated by overlaying the E2 molecules from the UbV.k.1−Ube2k and UbV.k.2−Ube2k structures with Ube2d2 from the RNF12−Ube2d2 crystal structure (PDB ID: 6W7Z). Only the Ube2k−UbV.k.1 complex is shown represented in a ribbon and semitransparent surface. The modeled RNF12 is shown as a green ribbon. (C) Ube2k in complex with UbV.k.1 with donor and acceptor ubiquitin molecules modeled at their predicted sites.[29]

containing a K97R mutation.[29,58] For all ubiquitin chain-building experiments, 5 μM E3 (RNF125, TRAF6, or RNF12), 0.1 μM E1, 8−10 μM E2 (Ube2k, Ube2d2, or Ube2n/Ube2v2), 50 μM ubiquitin, and 5 μM Ub-5AIF were incubated with or without 10−30 μM UbVs in a buffer containing 20 mM Tris-HCl (pH 7.5), 50 mM NaCl, 2 mM TCEP, 2 mM ATP, and 2 mM MgCl$_2$. Reactions were incubated at 37 °C and mixed with SDS loading dye containing 2-mercaptoethanol at the indicated time points. The resulting SDS-PAGE gels were imaged on a Las-3000 (Fuji Film) imager for approximately 60 s. For ubiquitin discharge assays, a purified thioester-linked Ube2k~Ub−Cy3^{K0} conjugate (approximately 2 μM) was mixed with 250 nM RNF125 or 2.5 μM RNF12 and 50 μM ubiquitin with or without UbVs at 10 μM and incubated at 20 °C. At the indicated time points, the samples were mixed with SDS loading dye containing no reducing agent and resolved with SDS-PAGE. Samples were imaged on an Odyssey FC imaging system (LI-COR) at 600 nm with a 2 min exposure. Charging assays of Ube2k were performed in PBS with 0.1 μM E1, 10 μM Ube2k, 50 μM ubiquitin, ±10 μM UbV.k.1 or UbV.k.2, 2 mM MgCl$_2$, and 2 mM ATP. Reactions were incubated at 37 °C before being mixed with nonreducing SDS dye, and proteins were visualized with Coomassie blue staining of the gels. E1 activation experiments were performed in PBS, 2 mM MgCl$_2$, 2 mM ATP with 0.5 μM E1, and 50 μM Ub-Cy3,

with or without 30 μM UbV.k.1 or UbV.k.2. The reactions were incubated at 20 °C for 5 min before being mixed with nonreducing SDS dye, and gels were resolved via fluorescence of Cy3 as for discharge experiments.

ELISA Experiments. For epitope mapping, 384-well high-binding plates (Greiner Bio-One) were coated overnight with streptavidin, GST, or GST−ubiquitin. Biotinylated Ube2k^k−UBC~Ub, Ube2k, or PBS was mixed with the immobilized streptavidin for ~15 min. Purified UbVs were then added at 0.5 μM, and binding was detected via reaction of 3,3′,5,5′-tetramethylbenzidine (TMB) with an HRP-FLAG antibody (1:4000, ThermoFisher Scientific). The colorimetric reaction was quenched with sulfuric acid after 5−10 min. Absorbance at 450 nm was measured with a ClarioSTAR Plus (BMG Labtech). The background was subtracted and values were normalized where the highest signal was 1.0. For the E2 specificity experiment in Figure 2A, we generated a representative pool of AVI-tagged and biotinylated E2 enzymes, immobilized these to streptavidin-coated plates, and assessed binding using a similar approach to that described above. For the EC$_{50}$ measurements, the UbVs were diluted as indicated before being mixed with Ube2k immobilized to streptavidin-coated plates. The EC$_{50}$ value is the concentration at which the signal of absorbance is 50% of total binding. These data were analyzed and plotted in R, version 4.0.4.

Binding Experiments. Isothermal titration calorimetry was performed with a VP-ITC (MicroCal) at 30 °C. Ube2k, Ube2k−UBC, and Ube2k^k−UBC∼Ub were added to the cell at 8, 8−10, and 7 μM, respectively, while UbV.k.1 (at 150 or 85 μM) and UbV.k.2 (at 110 μM) were in the syringe. All samples were either dialyzed against or purified with a common stock of PBS. Analysis was performed using NITPIC, SEDPHAT, and GUSSI.[59] Thermal denaturation of Ube2k was performed at a final protein concentration of 5 μM. SYPRO Orange (ThermoFischer) dye was added to the protein in a white 96-well PCR plate (Lab Supply) and measured in a Roche LightCycler 480 II instrument using the SYPRO Orange program. Data were analyzed and plotted with R, version 4.0.4.

Crystallography and Structure Solution. For crystallography, the copurified complexes were mixed with the crystal screens PACT Premier and JCSG plus (Molecular Dimensions) at 200:200 nL and 200:100 nL protein/well solution drop ratios in Swissci 3-well sitting drop plates using a mosquito (TTP Labtech). Diffraction-quality crystals of the UbV.k.2−Ube2k complex were produced in 0.2 M sodium citrate tribasic trihydrate, 0.1 M Bis-Tris propane at pH 7.5, and 20% (w/v) PEG 3350, and the data set was collected at the MX1 beamline, Australian Synchrotron. UbV.k.1−Ube2k^k∼Ub crystals were grown in 0.2−0.3 M ammonium citrate dibasic and 20−25% (w/v) PEG 3350, and data were collected at the MX2 beamline, Australian Synchrotron. Data were processed and scaled with XDS,[60] and data sets were merged with Aimless[61] from ccp4 v.7.1. Subsequently, Phaser-MR[62] was used to solve the structures using a single Ube2k molecule from PDB 5DFL[29] and the core domain of ubiquitin (PDB: 1UBQ).[63] For the UbV.k.1−Ube2k^k∼Ub data set, the ice ring at 3.4 Å was excluded from the processing. Both structures were refined with Phenix refine[64] (from Phenix v.1.19.1) and manually corrected iteratively using Coot v.0.9.5.[65] All images were generated using ChimeraX v.1.2.5.[66]

ASSOCIATED CONTENT

Ⓢ Supporting Information

The Supporting Information is available free of charge at https://pubs.acs.org/doi/10.1021/acschembio.1c00445.

Supporting figures and full gels (PDF)

Accession Codes

Crystal coordinates for UbV.k.1−Ube2k^k∼Ub and UbV.k.2−Ube2k have been deposited in the Protein Data Bank under accession codes 7MYF and 7MYH, respectively.

AUTHOR INFORMATION

Corresponding Author

Adam J. Middleton − *Department of Biochemistry, School of Biomedical Sciences, University of Otago, Dunedin 9054, New Zealand;* ⊙ orcid.org/0000-0002-6075-4061; Phone: +64 3 479 7870; Email: adam.middleton@otago.ac.nz

Authors

Joan Teyra − *The Donnelly Centre for Cellular and Biomolecular Research, University of Toronto, Toronto, Ontario M5S 3E1, Canada*

Jingyi Zhu − *Department of Biochemistry, School of Biomedical Sciences, University of Otago, Dunedin 9054, New Zealand*

Sachdev S. Sidhu − *The Donnelly Centre for Cellular and Biomolecular Research, University of Toronto, Toronto, Ontario M5S 3E1, Canada*

Catherine L. Day − *Department of Biochemistry, School of Biomedical Sciences, University of Otago, Dunedin 9054, New Zealand;* ⊙ orcid.org/0000-0003-1571-4367

Complete contact information is available at:

https://pubs.acs.org/10.1021/acschembio.1c00445

REFERENCES

(1) Hochstrasser, M. (1996) Ubiquitin-dependent protein degradation. *Annu. Rev. Genet. 30*, 405−39.

(2) Mark, K. G., and Rape, M. (2021) Ubiquitin-dependent regulation of transcription in development and disease. *EMBO Rep. 22*, e51078.

(3) Stewart, M. D., Ritterhoff, T., Klevit, R. E., and Brzovic, P. S. (2016) E2 enzymes: more than just middle men. *Cell Res. 26*, 423−440.

(4) Chen, Z. J. (2005) Ubiquitin signalling in the NF-κB pathway. *Nat. Cell Biol. 7*, 758−765.

(5) Pines, J. (2011) Cubism and the cell cycle: the many faces of the APC/C. *Nat. Rev. Mol. Cell Biol. 12*, 427−38.

(6) Rape, M. (2018) Ubiquitylation at the crossroads of development and disease. *Nat. Rev. Mol. Cell Biol. 19*, 59−70.

(7) Gundogdu, M., and Walden, H. (2019) Structural basis of generic versus specific E2-RING E3 interactions in protein ubiquitination. *Protein Sci. 28*, 1758−1770.

(8) Osborne, H. C., Irving, E., Forment, J. V., and Schmidt, C. K. (2021) E2 Enzymes in Genome Stability: Pulling the Strings Behind the Scenes. *Trends Cell Biol. 31*, 628.

(9) Dou, H., Buetow, L., Sibbet, G. J., Cameron, K., and Huang, D. T. (2012) BIRC7−E2 ubiquitin conjugate structure reveals the mechanism of ubiquitin transfer by a RING dimer. *Nat. Struct. Mol. Biol. 19*, 876−883.

(10) Koliopoulos, M. G., Esposito, D., Christodoulou, E., Taylor, I. A., and Rittinger, K. (2016) Functional role of TRIM E3 ligase oligomerization and regulation of catalytic activity. *EMBO J. 35*, 1204−18.

(11) Plechanovova, A., Jaffray, E. G., Tatham, M. H., Naismith, J. H., and Hay, R. T. (2012) Structure of a RING E3 ligase and ubiquitin-loaded E2 primed for catalysis. *Nature 489*, 115−20.

(12) Sanchez, J. G., Chiang, J. J., Sparrer, K. M. J., Alam, S. L., Chi, M., Roganowicz, M. D., Sankaran, B., Gack, M. U., and Pornillos, O. (2016) Mechanism of TRIM25 Catalytic Activation in the Antiviral RIG-I Pathway. *Cell Rep. 16*, 1315−1325.

(13) Scott, D. C., Sviderskiy, V. O., Monda, J. K., Lydeard, J. R., Cho, S. E., Harper, J. W., and Schulman, B. A. (2014) Structure of a RING E3 trapped in action reveals ligation mechanism for the ubiquitin-like protein NEDD8. *Cell 157*, 1671−84.

(14) Chen, Z., and Pickart, C. M. (1990) A 25-kilodalton ubiquitin carrier protein (E2) catalyzes multi-ubiquitin chain synthesis via lysine 48 of ubiquitin. *J. Biol. Chem. 265*, 21835−42.

(15) Djajawi, T. M., Liu, L., Gong, J., Huang, A. S., Luo, M., Xu, Z., Okamoto, T., Call, M. J., Huang, D. C. S., and van Delft, M. F. (2020) MARCH5 requires MTCH2 to coordinate proteasomal turnover of the MCL1:NOXA complex. *Cell Death Differ. 27*, 2484−2499.

(16) Hong, N. H., Tak, Y. J., Rhim, H., and Kang, S. (2019) Hip2 ubiquitin-conjugating enzyme has a role in UV-induced G1/S arrest and re-entry. *Genes Genomics 41*, 159−166.

(17) Kalchman, M. A., Graham, R. K., Xia, G., Koide, H. B., Hodgson, J. G., Graham, K. C., Goldberg, Y. P., Gietz, R. D., Pickart, C. M., and Hayden, M. R. (1996) Huntingtin is ubiquitinated and interacts with a specific ubiquitin-conjugating enzyme. *J. Biol. Chem. 271*, 19385−94.

(18) de Pril, R., Fischer, D. F., Roos, R. A., and van Leeuwen, F. W. (2007) Ubiquitin-conjugating enzyme E2−25K increases aggregate formation and cell death in polyglutamine diseases. *Mol. Cell. Neurosci. 34*, 10−9.

(19) Song, S., Kim, S. Y., Hong, Y. M., Jo, D. G., Lee, J. Y., Shim, S. M., Chung, C. W., Seo, S. J., Yoo, Y. J., Koh, J. Y., Lee, M. C., Yates, A. J., Ichijo, H., and Jung, Y. K. (2003) Essential role of E2−25K/Hip-2 in mediating amyloid-beta neurotoxicity. *Mol. Cell 12*, 553−63.

(20) Meiklejohn, H., Mostaid, M. S., Luza, S., Mancuso, S. G., Kang, D., Atherton, S., Rothmond, D. A., Weickert, C. S., Opazo, C. M., Pantelis, C., Bush, A. I., Everall, I. P., and Bousman, C. A. (2019) Blood and brain protein levels of ubiquitin-conjugating enzyme E2K (UBE2K) are elevated in individuals with schizophrenia. *J. Psychiatr. Res. 113*, 51−57.

(21) Su, J., Huang, P., Qin, M., Lu, Q., Sang, X., Cai, Y., Wang, Y., Liu, F., Wu, R., Wang, X., Jiang, X., Wang, J., Sun, Q., Chen, S., and Xu, J. (2018) Reduction of HIP2 expression causes motor function impairment and increased vulnerability to dopaminergic degeneration in Parkinson's disease models. *Cell Death Dis. 9*, 1020.

(22) Pluska, L., Jarosch, E., Zauber, H., Kniss, A., Waltho, A., Bagola, K., von Delbrück, M., Löhr, F., Schulman, B. A., Selbach, M., Dötsch, V., and Sommer, T. (2021) The UBA domain of conjugating enzyme Ubc1/Ube2K facilitates assembly of K48/K63-branched ubiquitin chains. *EMBO J. 40*, e106094.

(23) Ernst, A., Avvakumov, G., Tong, J., Fan, Y., Zhao, Y., Alberts, P., Persaud, A., Walker, J. R., Neculai, A.-M., Neculai, D., Vorobyov, A., Garg, P., Beatty, L., Chan, P.-K., Juang, Y.-C., Landry, M.-C., Yeh, C., Zeqiraj, E., Karamboulas, K., Allali-Hassani, A., Vedadi, M., Tyers, M., Moffat, J., Sicheri, F., Pelletier, L., Durocher, D., Raught, B., Rotin, D., Yang, J., Moran, M. F., Dhe-Paganon, S., and Sidhu, S. S. (2013) A Strategy for Modulation of Enzymes in the Ubiquitin System. *Science 339*, 590−595.

(24) Gabrielsen, M., Buetow, L., Nakasone, M. A., Ahmed, S. F., Sibbet, G. J., Smith, B. O., Zhang, W., Sidhu, S. S., and Huang, D. T. (2017) A General Strategy for Discovery of Inhibitors and Activators of RING and U-box E3 Ligases with Ubiquitin Variants. *Mol. Cell 68*, 456−470.e10.

(25) Teyra, J., Singer, A. U., Schmitges, F. W., Jaynes, P., Kit Leng Lui, S., Polyak, M. J., Fodil, N., Krieger, J. R., Tong, J., Schwerdtfeger, C., Brasher, B. B., Ceccarelli, D. F. J., Moffat, J., Sicheri, F., Moran, M. F., Gros, P., Eichhorn, P. J. A., Lenter, M., Boehmelt, G., and Sidhu, S. S. (2019) Structural and Functional Characterization of Ubiquitin Variant Inhibitors of USP15. *Structure 27*, 590−605.e5.

(26) Sidhu, S. S., Lowman, H. B., Cunningham, B. C., and Wells, J. A. [21] Phage display for selection of novel binding peptides. In *Methods Enzymol.*; Thorner, J., Emr, S. D., and Abelson, J. N., Eds.; Academic Press, 2000; pp 333−IN5.

(27) Merkley, N., and Shaw, G. S. (2004) Solution structure of the flexible class II ubiquitin-conjugating enzyme Ubc1 provides insights for polyubiquitin chain assembly. *J. Biol. Chem. 279*, 47139−47.

(28) Rennie, M. L., Chaugule, V. K., and Walden, H. (2020) Modes of allosteric regulation of the ubiquitination machinery. *Curr. Opin. Struct. Biol. 62*, 189−196.

(29) Middleton, A. J., and Day, C. L. (2015) The molecular basis of lysine 48 ubiquitin chain synthesis by Ube2K. *Sci. Rep. 5*, 16793.

(30) Krissinel, E., and Henrick, K. (2007) Inference of macro-molecular assemblies from crystalline state. *J. Mol. Biol. 372*, 774−97.

(31) Olsen, S. K., and Lima, C. D. (2013) Structure of a Ubiquitin E1-E2 Complex: Insights to E1-E2 Thioester Transfer. *Mol. Cell 49*, 884−896.

(32) Williams, K. M., Qie, S., Atkison, J. H., Salazar-Arango, S., Alan Diehl, J., and Olsen, S. K. (2019) Structural insights into E1 recognition and the ubiquitin-conjugating activity of the E2 enzyme Cdc34. *Nat. Commun. 10*, 3296.

(33) Middleton, A. J., Zhu, J., and Day, C. L. (2020) The RING Domain of RING Finger 12 Efficiently Builds Degradative Ubiquitin Chains. *J. Mol. Biol. 432*, 3790−3801.

(34) Buetow, L., Gabrielsen, M., Anthony, N. G., Dou, H., Patel, A., Aitkenhead, H., Sibbet, G. J., Smith, B. O., and Huang, D. T. (2015) Activation of a Primed RING E3-E2−Ubiquitin Complex by Non-Covalent Ubiquitin. *Mol. Cell 58*, 297−310.

(35) Ceccarelli, D. F., Tang, X., Pelletier, B., Orlicky, S., Xie, W., Plantevin, V., Neculai, D., Chou, Y.-C., Ogunjimi, A., Al-Hakim, A., Varelas, X., Koszela, J., Wasney, G. A., Vedadi, M., Dhe-Paganon, S., Cox, S., Xu, S., Lopez-Girona, A., Mercurio, F., Wrana, J., Durocher, D., Meloche, S., Webb, D. R., Tyers, M., and Sicheri, F. (2011) An Allosteric Inhibitor of the Human Cdc34 Ubiquitin-Conjugating Enzyme. *Cell 145*, 1075−1087.

(36) Maculins, T., Garcia-Pardo, J., Skenderovic, A., Gebel, J., Putyrski, M., Vorobyov, A., Busse, P., Varga, G., Kuzikov, M., Zaliani, A., Rahighi, S., Schaeffer, V., Parnham, M. J., Sidhu, S. S., Ernst, A., Dötsch, V., Akutsu, M., and Dikic, I. (2020) Discovery of Protein-Protein Interaction Inhibitors by Integrating Protein Engineering and Chemical Screening Platforms. *Cell Chem. Biol. 27*, 1441−1451.

(37) Garg, P., Ceccarelli, D. F., Keszei, A. F. A., Kurinov, I., Sicheri, F., and Sidhu, S. S. (2020) Structural and Functional Analysis of Ubiquitin-based Inhibitors That Target the Backsides of E2 Enzymes. *J. Mol. Biol. 432*, 952−966.

(38) Wang, H., Zhang, C., Rorick, A., Wu, D., Chiu, M., Thomas-Ahner, J., Chen, Z., Chen, H., Clinton, S. K., Chan, K. K., and Wang, Q. (2011) CCI-779 Inhibits Cell-Cycle G2−M Progression and Invasion of Castration-Resistant Prostate Cancer via Attenuation of UBE2C Transcription and mRNA Stability. *Cancer Res. 71*, 4866−4876.

(39) Wang, C., Shi, G., and Ji, X. (2018) Design, synthesis, and anticancer activity evaluation of irreversible allosteric inhibitors of the ubiquitin-conjugating enzyme Ube2g2. *MedChemComm 9*, 1818−1825.

(40) Liu, L., Hua, Y., Wang, D., Shan, L., Zhang, Y., Zhu, J., Jin, H., Li, H., Hu, Z., and Zhang, W. (2014) A Sesquiterpene Lactone from a Medicinal Herb Inhibits Proinflammatory Activity of TNF-*α* by Inhibiting Ubiquitin-Conjugating Enzyme UbcH5. *Chem. Biol. 21*, 1341−1350.

(41) Chen, H., Wu, G., Gao, S., Guo, R., Zhao, Z., Yuan, H., Liu, S., Wu, J., Lu, X., Yuan, X., Yu, Z., Zu, X., Xie, N., Yang, N., Hu, Z., Sun, Q., and Zhang, W. (2017) Discovery of Potent Small-Molecule Inhibitors of Ubiquitin-Conjugating Enzyme UbcH5c from *α*-Santonin Derivatives. *J. Med. Chem. 60*, 6828−6852.

(42) Helms, K. M., Wilson, R. C., Ogungbe, I. V., Setzer, W. N., and Twigg, P. D. (2011) Vitexin Inhibits Polyubiquitin Synthesis by the Ubiquitin-conjugating Enzyme E2−25K. *Nat. Prod. Commun. 6*, 1934578X1100601.

(43) Pulvino, M., Liang, Y., Oleksyn, D., DeRan, M., Van Pelt, E., Shapiro, J., Sanz, I., Chen, L., and Zhao, J. (2012) Inhibition of proliferation and survival of diffuse large B-cell lymphoma cells by a small-molecule inhibitor of the ubiquitin-conjugating enzyme Ubc13-Uev1A. *Blood 120*, 1668−1677.

(44) Cheng, J., Fan, Y.-H., Xu, X., Zhang, H., Dou, J., Tang, Y., Zhong, X., Rojas, Y., Yu, Y., Zhao, Y., Vasudevan, S. A., Zhang, H., Nuchtern, J. G., Kim, E. S., Chen, X., Lu, F., and Yang, J. (2014) A small-molecule inhibitor of UBE2N induces neuroblastoma cell death via activation of p53 and JNK pathways. *Cell Death Dis. 5*, e1079−12.

(45) Strickson, S., Campbell, D. G., Emmerich, C. H., Knebel, A., Plater, L., Ritorto, M. S., Shpiro, N., and Cohen, P. (2013) The anti-inflammatory drug BAY 11−7082 suppresses the MyD88-dependent signalling network by targeting the ubiquitin system. *Biochem. J. 451*, 427−437.

(46) Ardecky, R., Madiraju, C., Matsuzawa, S., Zou, J., Ganji, S., Pass, I., Ngo, T. A., Pinkerton, A. B., Sergienko, E., Su, Y., Stonich, D.,

Mangravita-Novo, A., Vicchiarelli, M., McAnally, D., Smith, L. H., Diwan, J., Chung, T. D. Y., Matsuzawa, Y., Wimer, C., Diaz, P. W., and Reed, J. C. Selective UBC 13 Inhibitors. In *Probe Reports from the NIH Molecular Libraries Program*; National Center for Biotechnology Information (US): Bethesda, MD, 2010.

(47) Cornwell, M. J., Thomson, G. J., Coates, J., Belotserkovskaya, R., Waddell, I. D., Jackson, S. P., and Galanty, Y. (2019) Small-Molecule Inhibition of UBE2T/FANCL-Mediated Ubiquitylation in the Fanconi Anemia Pathway. *ACS Chem. Biol. 14*, 2148−2154.

(48) Sanders, M. A., Brahemi, G., Nangia-Makker, P., Balan, V., Morelli, M., Kothayer, H., Westwell, A. D., and Shekhar, M. P. V. (2013) Novel Inhibitors of Rad6 Ubiquitin Conjugating Enzyme: Design, Synthesis, Identification, and Functional Characterization. *Mol. Cancer Ther. 12*, 373−383.

(49) Kothayer, H., Spencer, S. M., Tripathi, K., Westwell, A. D., and Palle, K. (2016) Synthesis and in vitro anticancer evaluation of some 4,6-diamino-1,3,5-triazine-2-carbohydrazides as Rad6 ubiquitin conjugating enzyme inhibitors. *Bioorg. Med. Chem. Lett. 26*, 2030−2034.

(50) Tokgoz, Z., Siepmann, T. J., Streich, F., Kumar, B., Klein, J. M., and Haas, A. L. (2012) E1-E2 Interactions in Ubiquitin and Nedd8 Ligation Pathways. *J. Biol. Chem. 287*, 311−321.

(51) Lv, Z., Rickman, K. A., Yuan, L., Williams, K., Selvam, S. P., Woosley, A. N., Howe, P. H., Ogretmen, B., Smogorzewska, A., and Olsen, S. K. (2017) S. pombe Uba1-Ubc15 structure reveals a novel regulatory mechanism of ubiquitin E2 activity. *Mol. Cell 65*, 699−714.e6.

(52) Bae, Y., Jung, S. H., Kim, G.-Y., Rhim, H., and Kang, S. (2013) Hip2 ubiquitin-conjugating enzyme overcomes radiation-induced G2/M arrest. *Biochim. Biophys. Acta, Mol. Cell Res. 1833*, 2911−2921.

(53) Liu, H., and Naismith, J. H. (2008) An efficient one-step site-directed deletion, insertion, single and multiple-site plasmid mutagenesis protocol. *BMC Biotechnol. 8*, 91.

(54) Sato, Y., Yoshikawa, A., Mimura, H., Yamashita, M., Yamagata, A., and Fukai, S. (2009) Structural basis for specific recognition of Lys 63-linked polyubiquitin chains by tandem UIMs of RAP80. *EMBO J. 28*, 2461−2468.

(55) Berndsen, C. E., and Wolberger, C. (2011) A spectrophotometric assay for conjugation of ubiquitin and ubiquitin-like proteins. *Anal. Biochem. 418*, 102.

(56) Middleton, A. J., Budhidarmo, R., Das, A., Zhu, J., Foglizzo, M., Mace, P. D., and Day, C. L. (2017) The activity of TRAF RING homo- and heterodimers is regulated by zinc finger 1. *Nat. Commun. 8*, 1788.

(57) Middleton, A. J., Budhidarmo, R., and Day, C. L. (2014) Use of E2~ubiquitin conjugates for the characterization of ubiquitin transfer by RING E3 ligases such as the inhibitor of apoptosis proteins. *Methods Enzymol. 545*, 243−63.

(58) Shin, D. Y., Lee, H., Park, E. S., and Yoo, Y. J. (2011) Assembly of different length of polyubiquitins on the catalytic cysteine of E2 enzymes without E3 ligase; a novel application of non-reduced/reduced 2-dimensional electrophoresis. *FEBS Lett. 585*, 3959−3963.

(59) Scheuermann, T. H., and Brautigam, C. A. (2015) High-precision, automated integration of multiple isothermal titration calorimetric thermograms: new features of NITPIC. *Methods 76*, 87−98.

(60) Kabsch, W. (2010) Xds. *Acta Crystallogr., Sect. D: Biol. Crystallogr. 66*, 125−32.

(61) CCP4 (1994) The CCP4 suite: programs for protein crystallography. *Acta Crystallogr., Sect. D: Biol. Crystallogr. 50*, 760−3.

(62) McCoy, A. J., Grosse-Kunstleve, R. W., Adams, P. D., Winn, M. D., Storoni, L. C., and Read, R. J. (2007) Phaser crystallographic software. *J. Appl. Crystallogr. 40*, 658−674.

(63) Vijay-Kumar, S., Bugg, C. E., and Cook, W. J. (1987) Structure of ubiquitin refined at 1.8 A resolution. *J. Mol. Biol. 194*, 531−44.

(64) Adams, P. D., Afonine, P. V., Bunkoczi, G., Chen, V. B., Davis, I. W., Echols, N., Headd, J. J., Hung, L. W., Kapral, G. J., Grosse-Kunstleve, R. W., McCoy, A. J., Moriarty, N. W., Oeffner, R., Read, R. J., Richardson, D. C., Richardson, J. S., Terwilliger, T. C., and Zwart, P. H. (2010) PHENIX: a comprehensive Python-based system for macromolecular structure solution. *Acta Crystallogr., Sect. D: Biol. Crystallogr. 66*, 213−21.

(65) Emsley, P., Lohkamp, B., Scott, W. G., and Cowtan, K. (2010) Features and development of Coot. *Acta Crystallogr., Sect. D: Biol. Crystallogr. 66*, 486−501.

(66) Pettersen, E. F., Goddard, T. D., Huang, C. C., Meng, E. C., Couch, G. S., Croll, T. I., Morris, J. H., and Ferrin, T. E. (2021) UCSF ChimeraX: Structure visualization for researchers, educators, and developers. *Protein Sci. 30*, 70−82.